Raman Spectroscopy and Structural Characteristics of Copper-Ion-Doped Silica Sol, Gel, and Aerogel

Mohammed A. Anaad[1], Israa F. Al-Sharuee[2,*]

1. Department of physics, College of Science, Al-Anbar University, Al-Anbar, Iraq.
2. Department of physics, College of Science, Mustansiriyah University, Baghdad, Iraq.

*Corresponding authors E-mail: i81f54@uomustansiriyah.edu.iq

Doi:10.29072/basjs.20230108

ARTICLE INFO

Keywords

Copper chloride; Doped aerogel; Raman spectrum; Silica gel; Spectral properties

ABSTRACT

This work presents the synthesis of silica sol, gel, and aerogel. To achieve a hydrophobic silica gel infused with copper chloride, a surface modification was performed on the sample. Furthermore, The present study focused on the examination of the evolutionary patterns of composition profiles in sol, gel, and aerogel materials. This investigation aimed to analyze the spectral properties of fluorescence, absorption, Raman spectroscopy, and FTIR spectrum. Additionally, the surface morphology, topography, and square of the surface roughness were evaluated using advanced imaging techniques such as scanning electron microscopy with a field-emission source (FE-SEM) and Atomic Force Microscope (AFM) images. The results indicate that there are notable distinctions in peak regions and distribution between the fluorescence and absorption spectra. This distinction is particularly evident in the Raman spectrum of sol, gel, and aerogel samples, where variations in peak regions and distribution are observed. Furthermore, the dominance of homogeneity and nano-structure, as well as the presence of surface roughness and increased surface area, are clearly discernible in the AFM topography.

Received 13 Mar 2023; Received in revised form 7 Apr 2023; Accepted 25 Apr 2023, Published 30 Apr 2023

1. Introduction

Silica-based compounds with broad applicability may be synthesized by the chemical process known as sol-gel synthesis[1, 2]. SiO_2 gel is usually made by catalyzing the polycondensation of tetra-alkoxysilanes (like TEOS or TMOS) in an alcoholic medium [3] However, the two-component non-aqueous sol-gel method is far less typical[4]. A strong carboxylic acid, such as formic acid, works as both a solvent and a catalyst by reacting directly with the silica precursor[5]. Ionic liquids (ionogels) are composites of silica and ionic liquids that have lately attracted a lot of interest due to their potential as materials for catalytic and electrolytic applications [6]. Most widely used and studied, silica aerogels exhibit remarkable qualities including high porosity (80-99.8%), high specific surface area (500-1200m^2 /g), very low conductivity (0.02W.m $^{-1}K^{-1}$) low density (0.003 g/cm^3), low index of refraction (1.05), and ultralow dielectric constant (k = (1.0-2.0)[7]. Because aerogels have these properties, they can be used for a wide range of things, such as sound and heat insulation, catalysis, electric devices, filtration, and collecting[8]. The industrial production of aerogels is mainly limited to silica-based systems, carbon, and some small amounts of organic aerogels [9]. Silica aerogels have recently gotten a lot of attention because they have unique properties and could be used in the future in a wide range of technical fields[10, 11]. Aerogel manufactured from silica has exceptional heat insulation qualities because to its nanostructure, high precise surface area, high porosity, low dielectric constant, tiny density, and lightweight[12, 13].In order to improve the strength and stiffness of the wet gel, aging it in a saline solution is necessary. Finally, a low surface tension solvent must replace the pore liquid to reduce drying shrinkage and capillary stress. [14]. The doping of aerogel has been utilized successfully in several reactions of catalytic oxidation. Strong impacts were recorded on the physical and chemical properties, such as account density, percentage of shrinkage, contact angle, thermal conductivity, and the optical transparency [15]. Many authors interested with improved the morphological and structural properties of silica aerogel via doping and add catalysis and discussed the results through Raman spectrum, FTIR, and AFM. This is done before the gel is dried, and the outcome is a polymer coating on the silica aerogel's surface, which significantly improves the material's breakage resistance. Yet, the use of fiber reinforcing procedures is the simplest approach to increase the strength of silica aerogel. The primary goal of incorporating short fibers into the silica aerogel structure, whether in a scattered or extended mat form, is to reinforce the structure. While silica aerogels have high structural characteristics and a moderate compressive strength, they are

exceedingly fragile [16].M.E. Krüger at. al, The findings demonstrate that an increase in Na/Si ratios leads to a lower degree of cross-linking because more non-bridging oxygens are present in the gel structure. Calcium contributes to a structural shift toward C-S-H phases in sodium-calcium silica gel they found. Raman spectroscopy shows promise as a tool for characterizing synthetic ASR gels they found and shedding light on how alkalis alter gel they found structure[17]. Wasan H. Al-husseny, at. al, Using HCl as a catalyst decreases the amount of water present in wet-gel they found which is the opposite of what happens if no HCl is added. The TEOS-based silica aerogel demonstrated the most similar properties to water glass, with the exception of transparency and gel they found time [18]. Dongxuan Du at. al, Fiber density's influence on SAC's thermal conductivity, mechanical qualities, and other physical characteristics is explored in depth. The findings reveal that at 10% strain, the compressive strength of SAC is 1.348 MPa and the thermal conductivity at 1100°C is 0.127 W/m K. SAC is anticipated to be employed as a useful and cost-effective insulating material because of its easy synthesis method and high thermal-mechanical performance [19]. J. Ben Naceur et al, analysis, structural and optical characteristics of sol-gel-they found processed TiO_2 thin films doped with iron ions (Fe3+). Raman spectroscopy and X-ray powder diffraction were used to examine how the crystalline phase changed with the addition of Fe, and spectrophotometer Ellipsometry spectroscopy was used to examine the Spin Coating process. Based on X-ray diffraction and Raman spectroscopy results, it seems that Fe ions either maintain the TiO_2 amorphous phase or restrict the crystallization process, depending on the concentration. As the concentration of TiO_2 was increased, the thin films' absorption edge moved from 356 to 416 nm, representing a change in wavelength [20]. Israa F. Al-Sharueez at. al, according to the findings, the aerogel's hydrophobic characteristic may be improved by the doping method. Doped aerogel has a lower density than undoped aerogel, meaning its particles are smaller and its surface is more uniform [21]. In this study, aerogels in ambient pressure are prepared and investigate the Raman and fluorescence and absorption spectrum in different cases as sol, gel, and aerogel. the investigation foxed on what the change in structural properties of samples and discuss the results.

2. Experimental procedure

Tetraethylorthosilicat (TEOS, 98 %) from Sigma-Aldrich, Germany. Trimethylchlorosilane (TMCS, > (98%) TCI Japan. Hexane (> 98%), from the Chem-Lab (Belgium). Schariau Ethanol (Spain) > (99%) Hydrochloric acid (35-38%), from Thoma Baker (India). Ammonia Solution from

CDH (India). Prepare the silica (sol, gel, modified gel, and aerogel doped with metal ions in (10^{-2}) gm/cm ^{3}, and dissolved copper chloride (Cu Cl) by add (0.085g) in(50ml) ethanol. In the first step Condensed silica (CS) as a precursor, TEOS was mixed with ethanol to create condensed silica with a molar ratio of TEOS (20ml) was mixed with (40ml) ethanol and on a magnetic stirrer for (10 minutes) and then (2ml) HCL [0.1M] as an acidic catalyst. Preparation stage sol(5ml) of copper chloride was mixed with (10ml) of condensed and then the each Add the base catalysis (0.5M NH_4OH) and stir in a magnetic field for 15 minutes to turn the sol into a gel. The gel is aged for two hours after being prepared for 15 minutes, then rinsed in ethanol three times every 24 hours. Surface modification was achieved by combining TMCS (7.5ml) with hexane (30ml). and applied to the gel put in the oven at (60℃) for 24hr. then it is placed in hexane soaked for 24hr. at room temperature, exchanged with pure hexane at (60℃) for 4hr. then exchanged with pure hexane at room temperature and washed in pure hexane and covered the holder in selofin with tiny holes and let them to dry at room temperature. put the gel in the oven at temperatures up about (180℃) gradually every 20 ℃ until they dry.

3. Characterizations of sol, gel, and aerogel

Raman spectroscopy is a technique that enables the measurement of molecular vibrations and phonons, hence offering valuable insights into the chemical composition, molecular conformation, and chemical structure of a given sample. Fourier Transform Infrared Spectroscopy (FTIR) Infrared spectroscopy is a specialized field within spectroscopy that focuses on the examination of the infrared area of the electromagnetic spectrum. This particular branch of spectroscopy enables the acquisition of valuable insights into the molecular composition of a given sample. By carefully evaluating the infrared absorption spectrum, pertinent information regarding the molecules present in the sample can be obtained. The purpose of this study is to examine the surface topography details, specifically focusing on the degree of surface roughness and the analysis of particle size. The atomic force microscope (AFM) is considered to be one of the contemporary technological advancements. Furthermore, it is employed for the purpose of determining the topography of surfaces characterized by nano and micro dimensions. This is accomplished by means of generating two- or three-dimensional pictures. The morphological structure and surface homogeneity of this sample were analyzed using field emission scanning electron microscopy (FESEM).

4. Results and discussion

4.1 Obtical Absorptions

Figure 1a and 1b depict the absorption spectrum observed for doped silica sol and gel, respectively. Absorbance measurements were conducted on the sol phase and the CuCl grafted gel phase, as depicted in two figures. During the sol phase, the absorbance exhibited a prominent peak at a wavelength of 270nm. Subsequently, the introduction of NH3OH resulted in a transformation of the sol into a gel state. A change in the absorbance value has been observed, with the maximum value occurring at a wavelength of 330nm. The phenomenon of brief positivity, characterized by high energies, is predominantly observed in the ultraviolet region, whereas its intensity diminishes in the visible ranges. This phenomenon can be attributed to the insufficient energy possessed by the descending photon, hence impeding its interaction with the atomic constituents. In instances where the wavelength is high, the photon will undergo displacement, hence resulting in an interaction between the photon and matter.

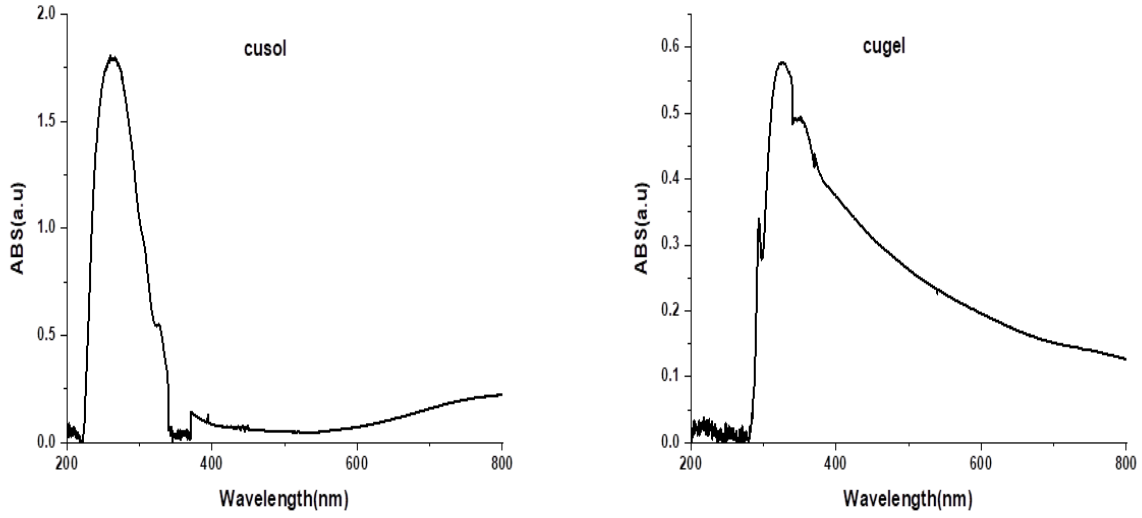

Figure 1: Absorption spectrum for doped silica (a):sol, (b): gel with CuCl.

4.2 Fluorescence spectrum

The fluorescence spectra of the prepared samples are depicted in Figure 2. The solution samples that were illuminated exhibited the greatest intensity at a wavelength of 430 nm. However, when these samples were converted into a gel, the highest intensity was observed at a wavelength of 450 nm. The findings of this study suggest that the presence of fluorescence can be ascribed to the chemical interactions between the probe particles and the hydroxyl radicals generated on the surface of the sol and gel via the photocatalytic reaction. Another possibility is that the fluorescent hydroxyl products are a result of the direct interaction between the photogenerated holes and the probe molecules. The gel appears to have high photocatalytic activity. This result is attributed to the high surface area and porosity of the photocatalyst particles. Fluorescence analysis of the hydroxyl products serves as an effective method for examining and demonstrating the potential reaction mechanism.

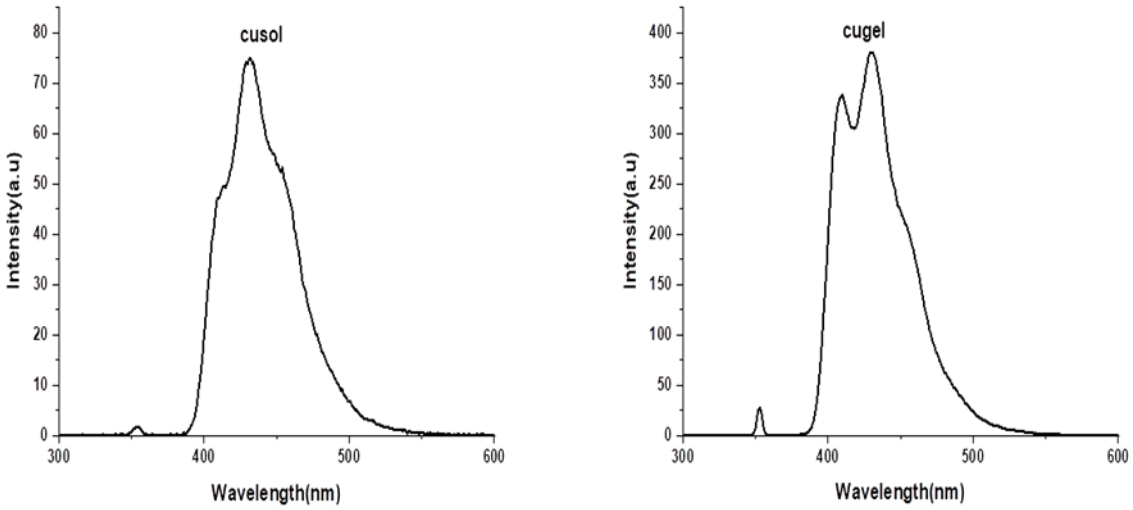

Figure 2: Fluorescence spectrum of doped silica (a):sol, (b): gel with CuCl.

4.3 Raman spectrum

The Raman spectra for each of the sol-phase reactants were obtained and are presented in Figure 3. The wavenumbers with the highest intensities are observed at 180.678 cm^{-1} and 688.375 cm^{-1}. The occurrence of tetraethyl orthosilicate (TEOS) functional groups results in the formation of Raman domains that are spatially proximate. By doing a comparative analysis of the conventional Raman spectra, it was possible to monitor the real-time progression of changes in the sol-gel process across different formulations. The objective is to determine the strengths of the primary components present in the 3-minute mixture. This includes the Si−O expansion mode of the silicon oxide located in the region 690.952. As can be seen, the silicon oxide molecules have a strong Raman peak in the region 180.375–688.375 cm^{-1} which corresponds to the stretching vibration of the Si $OCxH_2x + 1$ bond where the oxygen atom is attached to an alkyl group. The stronger Raman intensity of this peak relative to that in TEOS is attributed to the higher polarizability of the SiO bonds in the methyl-based precursor. In general, it is possible to distinguish major regions in the Raman spectroscopy of a copper chloride-doped antenna gel. We notice a shift in the Raman spectroscopy due to the drying of the sample at 180 $^{\circ}C$ degrees. The highest intensity appeared at wavelength 666.097-2113.214 nm for the aerogel prepared by surface modification using TMCS plus hexane, and this is due to the single type vibration represented by the symmetric stretching vibration, while for the lowest intensity peaks appeared at the next wavelength 3630.433-4330.878 nm. The appearance of these peaks of lower intensity is due to the symmetrical expansion vibration of two types of atoms. Table 1 presents a summary of the distinctive peaks observed for each chemical compound, along with their respective assignments, as determined from the spectra depicted in Figure 3.

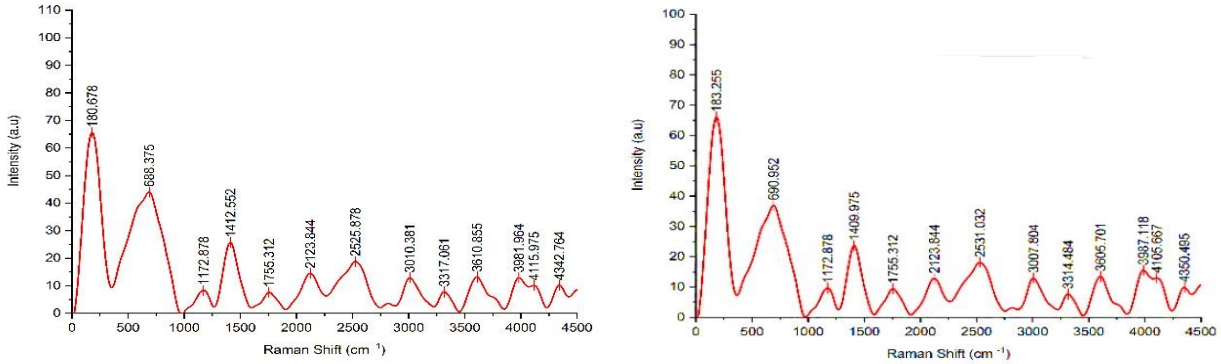

A. sol B. Gel

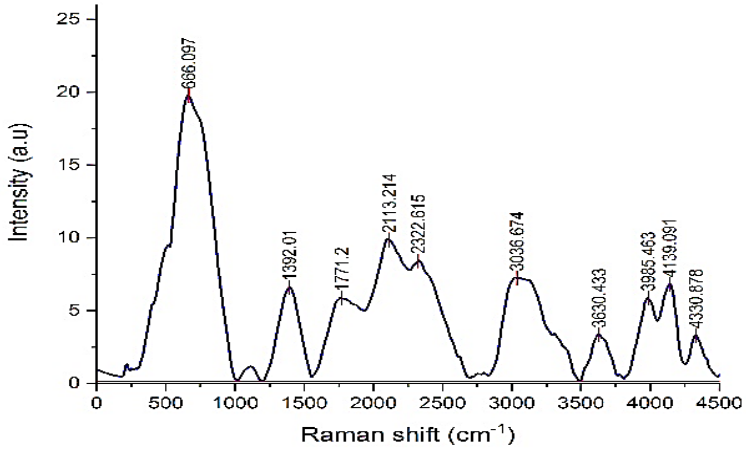

C. Aerogel

Figure 3: Raman spectrum of (a) sol, (b) gel, and (c) aerogel doped in CuCl

Table.1: The characteristic peaks and their corresponding assignments based on the Raman spectrum

Sol doped with CuCl			
X (cm^{-1})	**Y (a.u)**	**X (cm^{-1})**	**Y (a.u)**
180.678	65.61132	3010.381	12.92211
688.375	44.07824	3317.061	7.79919
1172.878	8.38281	3610.855	13.16917
1412.552	25.75841	3981.964	12.93383
1755.312	7.63706	4115.975	10.07445
2123.844	14.49945	4342.764	10.19555
2525.878	18.82629		
Gel doped with CuCl			
X (cm^{-1})	**Y (a.u)**	**X (cm^{-1})**	**Y (a.u)**
183.255	66.08088	3007.804	12.95934
690.952	36.96548	3314.484	7.65324
1172.878	9.68165	3605.701	13.50612
1409.975	23.67578	3987.118	15.55851
1755.312	9.46154	4105.667	12.96628
2123.844	12.84857	4350.495	9.91953
Aerogel doped with CuCl			
X ($cm^{-1)}$	**Y (a.u)**	**X (cm^{-1})**	**Y (a.u)**
666.097	19.74375	3036.674	7.23027
1392.01	6.58406	3630.433	3.34193
1771.2	5.86324	3985.463	5.8486
2113.214	9.85671	4139.091	6.8149
2322.615	8.41671	4330.878	3.2936

4.4 FTIR spectrum

Figure 4 represent the IR-spectrum for sol, gel and aerogel doped with CuCl.. This dip is less pronounced since the Si-O-Si bands at 1313 cm^{-1} and 460 cm^{-1} are present in all samples. Peaks at 3285, 1588, and 1013 cm^{-1} indicated that Si-CH_3 was being bent and stretched. H-OH peaks are also detected at 3556cm^{-1} and 1690 cm^{-1}. Additionally, the results show that the subsequent modification of TMCS/n-hexane greatly attenuates the signal ascribed to the Si-OH at 1160 cm^{1}Hydrophobic groups (alkyl) replaced hydrophilic ones (silanol groups) due to the potent influence of a changed solution. Also, this peak becomes stronger when non doped in metal ions, TMCS/n-hexane was successfully modified, as seen in the figure, and the surface modification was almost finished [32]. The Si-OH 1160 cm^{-1} peak has faded to the point that other peaks at 3556cm^{-1} and 1690 cm^{-1} have become evident, both of which may be ascribed to H-OH bands.

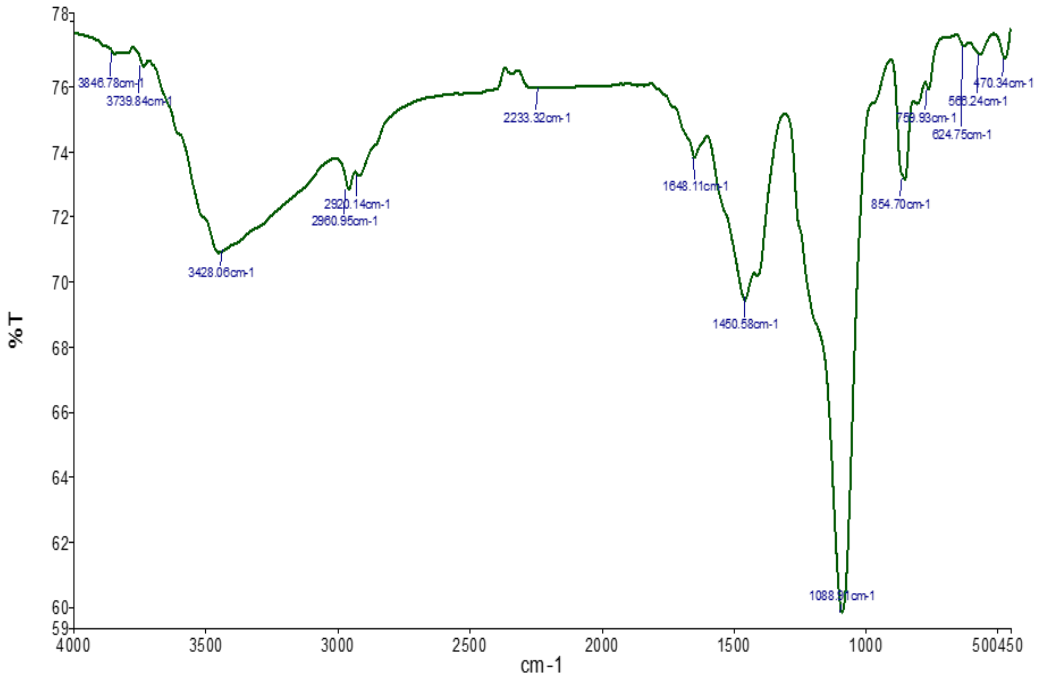

Figure 4: FTIR spectrum of doped silica aerogel with CuCl

4.5 Atomic Force Microscope (AFM)

The entire characterization of the nanostructure geometry is provided by the vertical and horizontal dimensions of the surface. The surface roughness factor holds significant importance as it serves

as an indicator of both surface quality and growth. The topic of discussion pertains to legumes. The highest height corresponds to the extent of nanoparticle expansion. The horizontal dimensions of the surface were ascertained using three-dimensional (3D) photographs of the comprehensive surface topography. The nanoparticles have unique capabilities due to their augmented surface area.

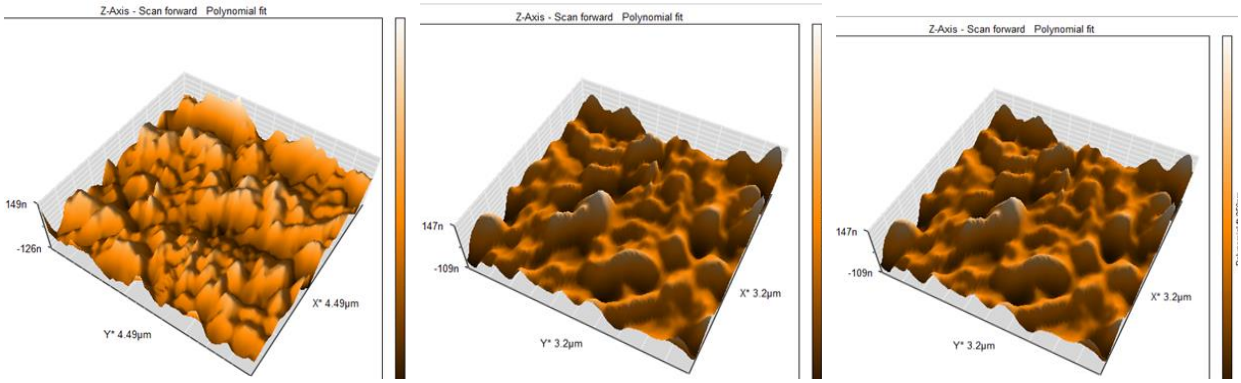

Figure 5: AFM images of doped silica aerogel with CuCl in different nanoscale.

From FESEM clear tiny pore size, along with the fact that the silica aerogel seems to be a continuous and densely cross-linked network, results in an extremely open structure in which individual particles are not distinguishable and the average particle size is rather large. By using a field emission scanning electron microscope, we were able to see the microstructure of the material (FESEM). When the silica aerogel particles are clumped together, they form aggregations with a smooth surface. There was also microstructural inhomogeneity, and the typical particle size was The image of showed the microstructure by field emission scanning electron microscope (FESEM).

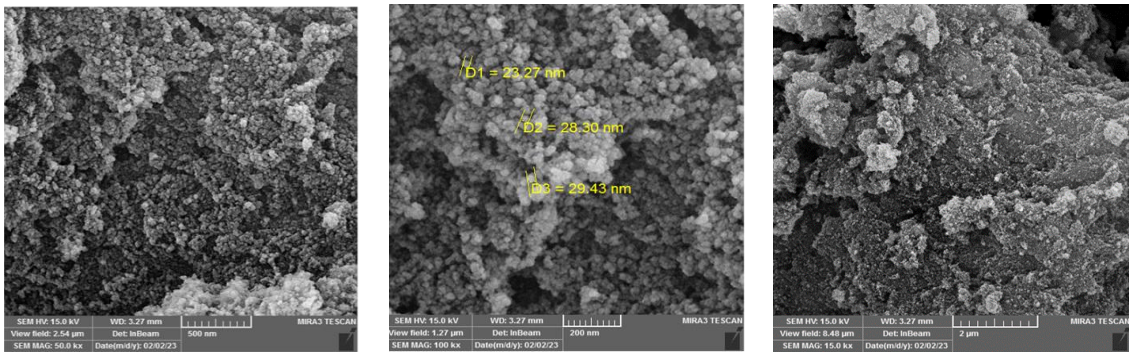

Figure 6: FESEM images of doped silica aerogel with CuCl in different magnification.

Conclusions

In summary, the nanoparticles were produced and doped utilizing the sol-gel-aerogel approach. The morphology of these particles was investigated using the Atomic Force Microscopy (AFM) technique. In instances where wavelengths are somewhat long, photons undergo a shift, resulting in an interaction between the absorbed photon and matter. The fluorescence phenomenon exhibits distinct variations in peak regions and distribution within the Raman spectrum when considering sol, gel, and aerogel materials. Additionally, the dominance of homogeneity and nano-structure is observed in these samples. The presence of microstructural heterogeneity was observed, with a notable disparity in the average particle size compared to the remaining particles. The microstructure was depicted in an image captured using a field emission scanning electron microscope (FESEM).

References

[1] R.Ciriminna, A Fidalgo, V. Pandarus, F. Beland, The sol–gel route to advanced silica- based materials and recent applications, Chem. Rev., 113(2013)6592-6620, https://doi.org/10.1021/cr300399c

[2] M. Kato, K. Sakai-Kato, T. Toyo'oka, Silica sol-gel monolithic materials and their use in a variety of applications, J. Sepa. sci., 28(2005)1893-1908, https://doi.org/10.1002/jssc.200500225

[3] Y. Özbakır, C. Erkey, Experimental and theoretical investigation of supercritical drying of silica alcogels, The J. Sup. Flu., 98 (2015) 153-166, https://doi.org/10.1016/j.supflu.2014.12.001

[4] C.J Brinker, G.W Scherer, Sol-gel science: the physics and chemistry of sol-gel processing, Acad. Pre.,2013,

[5] C.M. Golja, L.W Chew, J.A. Dykema, Aerosol dynamics in the near field of the SCoPEx stratospheric balloon experiment, J. of. Geop. Res. Atm., 126 (2021), https:// doi.org/10.1029/2020JD033438

[6] Z.L.Xie, H.B. Xu, A. Geßner, A transparent, flexible, ion conductive, and luminescent PMMA ionogel based on a Pt/Eu bimetallic complex and the ionic liquid [Bmim] [N (Tf)2], J. of. Mater. Chem., 22(2012)8110-8116, https://doi.org/10.1039/C2JM15862K

[7] D. Gu, F. Schüth, Synthesis of non-siliceous mesoporous oxides, Chem. Soci. Re., 43 (2014) 313-344,https:// doi. 10.1039/C3CS60155B

[8] A .Montes, MD. Gordillo, C. Pereyra, Silica microparticles precipitation by two processes using supercritical fluids,The J. Sup. Flu., 75 (2013) 88-93,https://doi.org/10.1016/j.supflu.2012.12.017

[9] I.Smirnova, P. Gurikov, Aerogels in chemical engineering: Strategies toward tailor-made aerogels, Ann. Rev. Chem. Biom. Eng., 8 (2017) 307-334, https://doi.org/10.1146/annurev-chembioeng-060816-101458

[10] T.Guo, S. Yun, Y. Li, Z. Chen, Facile synthesis of highly flexible polymethylsilsesquioxane aerogel monoliths with low density, low thermal conductivity and superhydrophobicity, Vac., 183(2021)109825, https://doi.org/10.1016/j.vacuum.2020.109825

[11] H.Maleki, Recent advances in aerogels for environmental remediation applications: A review, Chem. Eng. J., 300(2016) 98-118,https://doi.org/10.1016/j.cej.2016.04.098

[12] H.Cai, Y. Jiang, L. Li, J. Feng, Preparation of monodispersed silica sol with small particle size, narrow size distribution, and high conversion, J. Sol-Gel Sci. Tec., 91(2019) 44-53,https://doi.org/10.1007/s10971-019-05025-z

[13] W.Hu, M. Li, W. Chen,Preparation of hydrophobic silica aerogel with kaolin dried at ambient pressure. Colloids and Surfaces A: Physicochemical and Engineering Aspects, 501(2016) 83-91, https:// doi.org/10.1016/j.colsurfa.2016.04.059

[14] J.P.Nayak, J .Bera, Preparation of silica aerogel by ambient pressure drying process using rice husk ash as raw material, Tran. C. of. the Ind. Cer. Soc., 68(2009) 91-94, https://doi.org/10.1080/0371750X.2009.11082163

[15] Z. Chen, Y. Zhao, X. Zhu, Inclusion of hydrophobic liquids in silica aerogel microparticles in an aqueous process: microencapsulation and extra pore creation, ACS. Appl.Mater. & Int., 13 (2021) 12230-12240, https://doi.org/10.1021/acsami.1c00205

[16] X.Tang, A .Sun, C. Chu, M .Yu, A novel silica nanowire-silica composite aerogels dried at ambient pressure, Mater. & Design., 115(2017) 415-421, https://doi.org/10.1016/j.matdes.2016.11.080

[17] M .Krüger, V Thome, H Hilbig, Investigations on alkali-silica reaction products using Raman spectroscopy, Mater. de. Con., 72(2022) e281-e281, https://.doi.org/10.3989/mc.2022.15621

[18] U. Berardi, S.M Zaidi, Characterization of commercial aerogel-enhanced blankets obtained with supercritical drying and of a new ambient pressure drying blanket. Ener. Build., 198 (2019) 542-552, https://doi.org/10.1016/j.enbuild.2019.06.027

[19] D. Du, F. Liu, Y. Jiang, Facile Preparation of High Strength Silica Aerogel Composites via a Water Solvent System and Ambient Pressure Drying without Surface Modification or Solvent Replacement, Mater., 14(2021) 3983, https://doi.org/10.3390/ma14143983

[20] JB. Naceur, R. Mechiakh, F. Bousbih, Influences of the iron ion (Fe3+)-doping on structural and optical properties of nanocrystalline TiO_2 thin films prepared by sol–gel spin coating, Appl. Sur. Sci., 257(2011)10699-10703, https://doi.org/10.1016/j.apsusc.2011.07.082

[21] I.F.Al-Sharueez, W.A. Twej, Study the Effect of Doping with Chromium Chloride on Silica Aerogel Properties Prepared with Ambient Pressure, J. Appl. Phys. (IOSR-JAP)., 9(2017) 28-32,https:// doi: 10.9790/4861-0903012832

التحليل الطيفي لرامان والخصائص الهيكلية للسيليكا المطعم بالنحاس سول، هلام، والهلام الهوائي

محمد اسعد عناز[1] واسراء فاخر الشرع[2]

1 قسم الفيزياء كلية العلوم جامعة الانبار

2 قسم الفيزياء كلية العلوم الجامعة المستنصرية

المستخلص

في هذا البحث، تم تصنيع السيليكا سول، والهلام، والهلام الهوائي. وإجراء تعديل على سطح العينة، للحصول على هلام السيليكا المقاوم للماء مطعم بكلوريد النحاس. كما تمت مناقشة تطور التشكيلات الجانبية للتكوين داخل محلول السول والهلام والهلام الهوائي لتوفير الخصائص الطيفية الفلورة والامتصاص والتحليل الطيفي لرامان وطيف FTIR وفحص مورفولوجيا السطح وتضاريسه ومربع خشونة السطح باستخدام المجهر الإلكتروني الماسح بمصدر انبعاث ميداني (FE-SEM) وصور مجهر القوة الذرية (AFM).أظهرت النتائج أن طيف التألق والامتصاص يشير إلى مزيد من الاختلاف في مناطق القمم والتوزيع، وكانت هذه النتائج واضحة جدًا في طيف رامان في حالة عينات سول والهلام والهلام الهوائي، من خلال الاختلاف في مناطق القمم والتوزيع، بالإضافة إلى التجانس. الهيكل النانوي هو المسيطر، بالإضافة إلى خشونة السطح وزيادة مساحة السطح واضحة ف